# The Coulomb four-body problem in a classical framework: triple photoionization of lithium

**Agapi Emmanouilidou**[1] **and Jan M Rost**[2]

[1] School of Physics, Georgia Institute of Technology, Atlanta, GA 30332-0430, USA
[2] Max Planck Institute for the Physics of Complex Systems, D-01187 Dresden, Germany

## Abstract

Formulating a quasiclassical approach we determine the cross section for the complete four-body break-up of the lithium ground state following single photon absorption from threshold up to 220 eV excess energy. In addition, we develop a new classification scheme for three-electron ionizing trajectories in terms of electron–electron collisions, thereby identifying two main ionization paths which the three electrons in the ground state of lithium follow to escape to the continuum. The dominant escape paths manifest themselves in a characteristic 'T-shape' break-up pattern of the three electrons which implies observable structures in the electronic angular correlation probability. This break-up pattern prevails for excess energies so low that the Wannier threshold law $\sigma \propto E^\alpha$ describes already the triple ionization cross section, whose predicted value $\alpha = 2.16$ we can confirm quantitatively.

## 1. Introduction

The broad interest in multi-electron photoionization processes is due to the fundamental role they play for understanding electron correlation induced by long-range Coulomb forces. Identifying the different paths the electrons follow to escape to the continuum is essential in uncovering a variety of fundamental phenomena, from pattern in highly differential cross sections over interference phenomena to the energy dependence of the total ionization cross section. The theoretical treatment of multiple ionization processes is highly complex with no analytic solution. In the energy domain, the difficulty is that one has to account for the correlated motion of the electrons in the asymptotic form of the final continuum state. In the time domain, this difficulty can be avoided at the expense of propagating the fully coupled few-body Coulomb problem in time.

For three electrons and sufficiently high photon energies this has been achieved in [1] and for even higher energies one may use approximate schemes [2]. Experimentally, the first data on triple ionization appeared only recently [3, 4], compared to data on photo double ionization which date back to the late sixties of the last century [5].

In the current work, we present a theoretical study of the total triple ionization cross section of lithium over a wide range in energy, from threshold up to 220 eV excess energy, and predict characteristic features in the electronic angular correlation probability. While the total triple ionization cross section has already been measured [3] and compares favourably with our results, the electronic angular correlation probability is not known experimentally. However, it should be measurable with state of the art experimental techniques.

Given the obstacles in the theoretical description stated above we are only able to achieve these results by formulating the four-body break-up process quasiclassically. This implies classical propagation of the Coulomb four-body problem using the classical trajectory Monte Carlo (CTMC) phase space method. CTMC has often been used to describe break-up processes induced by particle impact [6–9] with implementations differing usually in the way the phase space distribution of the initial state is constructed. We use a Wigner transform of the initial quantum wavefunction for the initial state, and this is why we call our approach 'quasi'-classical. Naturally, the electron–electron interaction is treated to all orders in the propagation, and any difficulties with electron correlation in the final state are absent, since the method is explicitly time dependent.

While the classical results follow from a large numerical effort, they still allow for a detailed analysis of the trajectories in terms of their physical properties. We will demonstrate that the triply photoionizing trajectories can be organized in groups according to the respective sequence of electron–electron collisions. From the emerging scheme we identify two main paths that lead to triple ionization from the Li ground state. The group to which an ionizing trajectory belongs is identified in an automated process which warrants a transfer of the classification scheme to more than three-electron atoms without technical difficulties. Physically, the nature of the collision scheme also promises a generalization to more electrons.

Furthermore, being quasiclassical, our approach naturally addresses the energy regime close to threshold. This energy regime has been traditionally of particular interest since the slow electron escape allows for large interaction times resulting in pronounced interactions among the escaping electrons. We could confirm the Wannier threshold law $\sigma \propto E^\alpha$ for the four-body break-up of lithium by single photon absorption with $\alpha = 2.16$ in the energy range of 0.1–2 eV as detailed in [10].

The paper is organized as follows: in section 2 we explain the theoretical approach, in section 3 we present the most important results, the triple ionization cross section and the electronic angular correlation probability. Section 4 introduces the classification scheme of ionizing trajectories which can explain the electronic angular correlation probability in terms of the dominant 'T-shaped' pattern of the three escaping electrons. Section 5 is dedicated to a final discussion and a summary.

## 2. Quasiclassical theory of photoionization

We formulate the triple photoionization process from the Li ground state ($1s^2 2s$) as a two-step process [2, 11, 12]. First, one electron absorbs the photon (photo-electron). Then, due to the electronic correlations, redistribution of the energy takes place resulting in three electrons escaping to the continuum. We express the above two-step process as

$$\sigma^{3+} = \sigma_{abs} P^{3+}, \tag{1}$$

where $\sigma_{abs}$ is the total absorption cross section and $P^{3+}$ is the probability for triple ionization. In what follows, we evaluate $P^{3+}$ and use the experimental data of Wehlitz [13] for $\sigma_{abs}$. Equally well, we could use a theoretically calculated $\sigma_{abs}$ [14] which is easy to obtain following the approach of [15]. To compute $P^{3+}$, we first assume that the photo-electron is a 1s-electron.

It absorbs the photon at the nucleus ($\mathbf{r}_1 = 0$), an approximation that becomes exact in the limit of high photon energy [16] and is in analogy to the successful description of photo double ionization in two-electron atoms [12]. The photon could also be absorbed by the Li 2s-electron. However, the cross section for photon absorption from a 1s orbital is much larger than from a 2s orbital as investigated in [17] for photoionization of an excited He(1s2s) atom. Hence, we can safely assume that the photo-electron is a 1s electron which significantly reduces the initial phase space to be sampled. Also, by virtue of their different character the electrons become practically distinguishable and allow us to neglect antisymmetrization of the initial state. We denote the photo-electron by 1, the other 1s electron by 2 and the 2s electron by 3. Immediately after photon absorption, we model the initial phase space distribution of the remaining two electrons, 1s and 2s, by the Wigner transform of the corresponding initial wavefunction $\psi(\mathbf{r}_1 = 0, \mathbf{r}_2, \mathbf{r}_3)$, where $\mathbf{r}_i$ are the electron vectors starting at the nucleus. We approximate the initial wavefunction as a simple product of hydrogenic orbitals $\phi_i^{Z_i}(\mathbf{r}_i)$ with effective charges $Z_i$, to facilitate the Wigner transformation. The $Z_i$ are chosen to reproduce the known ionization potentials $I_i$, namely for the 2s electron $Z_3 = 1.259$ ($I_3 = 0.198$ au) and for the 1s electron $Z_2 = 2.358$ ($I_2 = 2.780$ au). (We use atomic units throughout the paper if not stated otherwise.) The excess energy, $E$, is given by $E = E_\omega - I$ with $E_\omega$ the photon energy and $I = 7.478$ au the Li triple ionization threshold energy. For a given $E$, the Wigner distribution $W$ has an energy spread and it is only its expectation value that is equal to $E$ [18]. Since near $E = 0$ energy conservation is vital we enforce it by restricting the Wigner functions for the individual electron orbitals to their respective energy shell[3]. Following these considerations, the initial phase space distribution is given by

$$\rho(\Gamma) = \mathcal{N}\delta(\mathbf{r}_1)\delta(\varepsilon_1 + I_1 - \omega) \prod_{i=2,3} W_{\phi_i^{Z_i}}(\mathbf{r}_i, \mathbf{p}_i)\delta(\varepsilon_i + I_i) \tag{2}$$

with normalization constant $\mathcal{N}$ and the Wigner function defined as

$$W_{\phi^Z}(\mathbf{r}, \mathbf{p}) = (2\pi)^{-3} \int [\phi^Z(\mathbf{r} - \mathbf{x}/2)]^* \phi^Z(\mathbf{r} - \mathbf{x}/2) \exp(-i\mathbf{p}\mathbf{x}) \, d\mathbf{x} \tag{3}$$

for the hydrogenic wavefunctions $\phi^Z$ with effective charge $Z$.

We determine the triple ionization probability $P^{3+}$ formally through

$$P^{3+} = \lim_{t \to \infty} \int_{t_{abs}}^{t} d\Gamma_{\mathcal{P}^{3+}} \exp((t - t_{abs})\mathcal{L}_{cl})\rho(\Gamma), \tag{4}$$

where $t_{abs}$ is the time of photoabsorption and the classical Liouvillian $\mathcal{L}_{cl}$ defines the classical evolution of any phase space distribution $\mathbf{A}(\Gamma, t)$ with phase space vectors $\Gamma = (x_1, \ldots, x_n, p_1, \ldots, p_n)^\dagger$ through

$$\mathcal{L}_{cl}\mathbf{A} = \{H(\Gamma), \mathbf{A}(\Gamma, t)\} = \nabla H(\Gamma) \cdot [\mathbf{J}\nabla A(\Gamma, t)] \tag{5}$$

leading to [20, 21]

$$\mathbf{A}(\Gamma, t) = \exp((t - t_0)\mathcal{L}_{cl})\mathbf{A}(\Gamma, t_0). \tag{6}$$

Here, $\mathbf{J}$ is the symplectic matrix [21] with the help of which Hamilton's equations of motion can be written as

$$\dot{\Gamma} = \mathbf{J}\nabla H(\Gamma), \qquad \Gamma(t_0) = \Gamma_0. \tag{7}$$

The projector $\mathcal{P}^{3+}$ restricts the integration to those parts of phase space that lead to triple ionization [22]. Equation (4) amounts to propagating electron trajectories using the classical equations of motion (CTMC). Regularized coordinates [23] are used to avoid problems with electron trajectories starting at the nucleus. We evaluate $P^{3+}$ by weighting each triply ionized trajectory by the initial phase space distribution and adding the contributions [12].

---

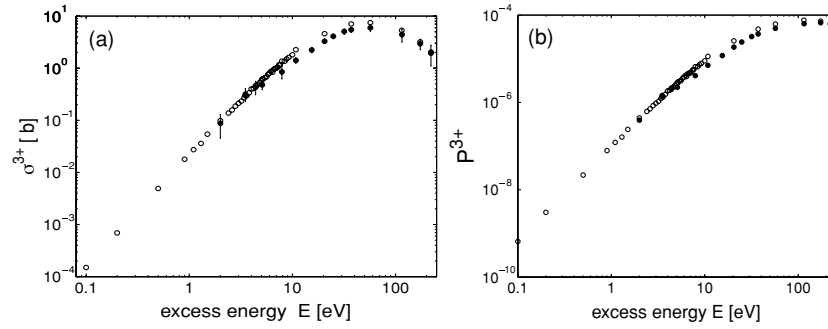[3] For the physical reasons for restricting $W$ in energy space in the context of the CTMC method see [8].

**Figure 1.** (a) Triple photoionization cross section obtained by multiplying the triple photoionization probability from the present calculation (○) with the total photo cross section from [13] in comparison to the experiment [3, 4] (experimental results (●) shown with error bars). (b) Shows triple photoionization probability $P^{3+}$ as a function of excess energy: present calculation (○); experiment (●) [3, 4, 13].

## 3. Experimentally accessible observables: total triple photoionization and angular correlation probability

Observables calculated classically or semiclassically tend to better approximate the 'exact' value if they represent a quantity averaged over as many degrees of freedom as possible. The reason for this is that classically forbidden mechanisms such as tunnelling and pronounced interference effects are less likely to play a prominent role if the dynamics is averaged over many degrees of freedom. Secondly, for classical calculations based on Monte Carlo methods, one 'counts' events, similarly as in the experiment. This means, only (randomly sampled) trajectories, whose final phase space values fall into a certain bin, contribute to the observable. As in the experiment, statistics of the contribution is an important factor and therefore, more integrated observables are easier to determine compared to highly differential ones. Interestingly, the classical domain of validity is complementary to that of approximate quantum calculations, e.g., with the so-called 6C wavefunction [24] where the fully differential cross section is calculated and more integrated observables require numerically expensive integrations.

For the present case, this implies that our focus is the triple ionization cross section (which is the 'most integrated' three-electron observable) with our statistics also allowing the evaluation of single differential cross sections. Here, we present for reasons which will become clear in section 3 an unusual but observable quantity, the electronic angular correlation probability, which answers the question: How likely is it in triple ionization to find two electrons under a certain angle $\theta$?

### 3.1. Triple photoionization cross section

We have already described in section 2 how to determine the triple photoionization cross section $\sigma^{3+}$ which is shown in figure 1(a). Note that no fitting parameters are used to obtain $\sigma^{3+}$. However, one may object that we use the total photo cross section extracted from another calculation or the experiment for the curve in figure 1(a). Hence we present in figure 1(b) the triple ionization probability $P^{3+}$ which we calculate directly and which can also be obtained directly from experimental data using the relation

$$P^{3+} = R^{3+}/(1 + R^{2+} + R^{3+}), \tag{8}$$

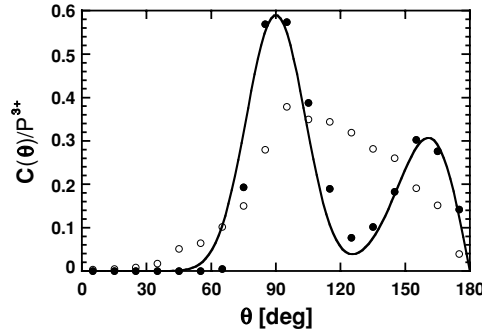**Figure 2.** The angular correlation probability $C(\theta)/P^{3+}(E)$ defined in (9) for $E = 0.9$ eV ($\bullet$) and for $E = 220.5$ eV ($\circ$), normalized to the respective triple ionization probability ($P^{3+}(E = 0.9$ eV$) = 7.89 \times 10^{-8}$, $P^{3+}(E = 220.5$ eV$) = 6.43 \times 10^{-5}$)). The number of events $N$ has been binned over $10°$ at $\theta_j = 5° + j10°$, $j = 0, 1, \ldots, 17$. For the solid line, see section 4.3.

where $R^{3+}$ and $R^{2+}$ are the experimental triple-to-single and double-to-single photoionization ratios, respectively [3, 4, 13]. Figure 1(b) also illustrates the numerical effort involved in computing $P^{3+}$. For example, to obtain $10^3$ triple photoionizing trajectories at $E = 0.9$ eV with $P^{3+} \sim 10^{-7}$ one has to evolve $10^{10}$ trajectories with the CTMC method [6].

Considering the approximations we had to make to handle the four-body problem, the agreement with the experimental data is remarkably good, starting near threshold where we can confirm the classically expected behaviour of the cross section [10] according to Wannier's theory [25, 26]. The agreement extends beyond the maximum of the cross section where our results also agree with the data points recently obtained in an *ab initio* calculation [1]. Hence, our classical approach with an approximate initial quantum wavefunction apparently captures the relevant correlations among the three electrons. For very high excess energies (currently not considered) the triple photoionization cannot be adequately described by our quasiclassical formulation. However, one can describe the process using the Born approximation.

### 3.2. Angular correlation probability

As already indicated, with only $10^3$ triple ionization events out of $10^{10}$ trajectories, at most a single differential observable can be determined. Interesting with respect to dynamical correlation among the three electrons and experimentally accessible is the angular correlation probability

$$C(\theta) = \lim_{t \to \infty} \sum_{i > j = 1}^{3} \int_{t_{\text{abs}}}^{t} d\Gamma_{\mathcal{P}^{3+}} \exp((t - t_{\text{abs}})\mathscr{L}_{\text{cl}})\rho(\Gamma)\delta(\theta_{ij}(t) - \theta), \tag{9}$$

with

$$\theta_{ij}(t) = \arccos[\mathbf{p}_i(t)\mathbf{p}_j(t)/(p_i(t)p_j(t))], \tag{10}$$

which depends only on the *relative* angle $\theta_{ij}$ between any pair of ionized electrons in the three electron escape. Formally, this is easily achieved within a CTMC approach. However, the number of events is very small and we need to bin the observable over $10°$ respectively, as shown in figure 2. We see for the higher excess energy ($E = 220.5$ eV) a broad distribution with a maximum near $90°$. This might have been expected from impulsive binary collisions of the fast photo-electron (peak at $\theta = 90°$) where the shift to slightly larger $\theta$ indicates the (small)

influence of the Coulomb repulsion. At $E = 0.9$ eV, the situation is drastically different: a double-hump structure emerges with peaks at $90°$ and $180°$.[4] This can be interpreted as 'T-shaped' structure which the three outgoing electrons form, where two of them leave along a line towards opposite sides and the third one leaves perpendicularly to the line. The origin of this double-hump structure and its interpretation as a T-shape configuration of the escaping electrons will become clear after the analysis of the electron collision sequences in the next section.

## 4. Classification of triple ionization dynamics in terms of an electron–electron collision scheme

### 4.1. The definition of electron collisions in a multi-electron system

The (dipole) coupling to the electromagnetic field is a single-electron operator. Hence, one electron absorbs the photon, which gets thereby annihilated. Before this photo-electron has left the atom it must transfer part of its energy to the other electrons to be ionized within a very short time. How this happens, directly or indirectly, is a question which is difficult to ask quantum mechanically, but is a natural question in classical mechanics, where the electrons undergo soft collisions mediated by Coulomb forces. In contrast to billiard balls they can indeed transfer energy among themselves if the nucleus is within the reach of the Coulomb potential to absorb the recoil momentum. Moreover, in a two-electron atom, it is most likely that a single collision among the two electrons occurs which does not provide a lot of insight. However, in three-electron atoms, the situation is far more complex and *a priori* the nature of the collisions is not clear: Is triple ionization mediated mostly by a single collision involving all three electrons or does it happen sequentially with a sequence of momentum transferring two-electron collisions? If the latter is the case, is there a pattern of preferred sequences? Does a characteristic collision pattern of classical trajectories leads to observable consequences?

Before we can answer these questions we first have to define what we call a momentum transferring electron–electron collision along a trajectory with time-dependent electron positions $\mathbf{r}_i(t)$, $i = 1, 2, 3$. The term responsible for momentum transfer between electrons $i$ and $j$ is their Coulomb repulsion $V(r_{ij}) = r_{ij}^{-1}$, $\mathbf{r}_{ij} = \mathbf{r}_i - \mathbf{r}_j$. Hence, we identify a collision between electrons $i$ and $j$ ($j$) through the momentum transfer

$$\mathbf{D}_{ij} := - \int_{t_1}^{t_2} \nabla V(r_{ij}) \, \mathrm{d}t \tag{11}$$

under the condition that $V(r_{ij}(t_k))$, $k = 1, 2$ are local minima in time with $t_2 > t_1$, while $r_{ij} = |\mathbf{r}_i - \mathbf{r}_j|$. This automatically ensures that the integral of (11) includes the 'collision' with a local maximum of $V(r_{ij}(t_k))$ at a time $t_1 < t_M < t_2$. During the time interval $t_1 < t < t_2$, all four particles interact with each other. Hence, the definition (11) is only meaningful if the collision redistributes energy dominantly within the subsystem given by the two-electron Li$^+$-Hamiltonian H$_{ij}$ of the nucleus and the electrons $i$ and $j$ involved in the actual collision. This is indeed the case since the energy in the subsystem H$_{ij}$ changes little over the collision, i.e., $\int_{t_1}^{t_2} \mathrm{d}H_{ij}/\mathrm{d}t \, \mathrm{d}t \ll E$, where $E$ is the total energy of the Li-Hamiltonian. We illustrate the latter statement in figure 3 using as an example a triple ionizing trajectory labelled by the sequence of (12, 13) electron–electron collisions. During the 12 collision (see figure 3(a)), $V(r_{12})$ undergoes a sharp change while H$_{12}$ changes smoothly. Thus, during the 12 collision, the $V(r_{12})$ potential energy is primarily redistributed in the Li$^+$ subsystem of electrons 1 and 2.

---

[4] Convolution with the volume element $\sin \theta$ leads to an appearance of the $180°$–peak at a smaller angle, see section 4.3.
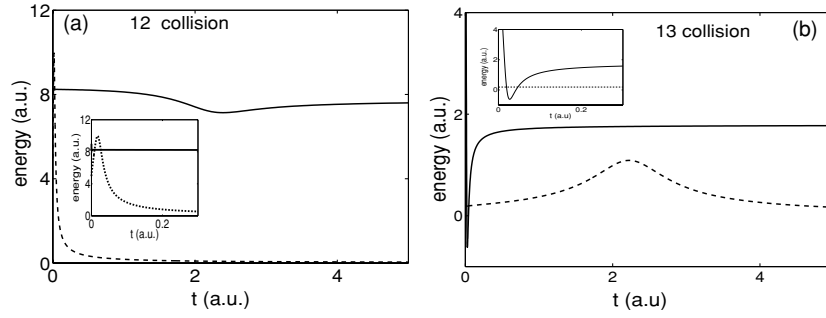
**Figure 3.** Energies in time for three-body subsystems for a triple ionizing trajectory with (12, 13) electron–electron collision sequence at $E = 220.5$ eV. The maxima of $V(r_{12})$ and $V(r_{13})$ occur at times 0.017 au (0.41 as) and 2.22 au (54 as), respectively. In (a) the solid line is the energy of the $H_{12}$ subsystem, while the dashed line is the interaction $V(r_{12})$. In (b) the solid line is the energy of the $H_{13}$ subsystem, while the dashed line is $V(r_{13})$. The insets are for short times $t$.
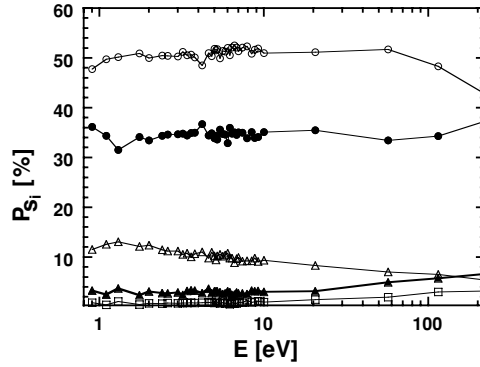


**Figure 4.** Probability relative to all triple ionizing trajectories classified according to the sequence $s_i$ of electron–electron collision $ij$, see the text; $s_1 = (12, 13)$ ($\circ$), $s_2 = (12, 23)$ ($\bullet$), $s_3 = (13, 12)$ ($\square$), $s_4 = (12, 13, 23)$ ($\triangle$), $s_5 = (23, 12, 13)$ ($\blacktriangle$).

Similarly, during the 13 collision (see figure 3(b)), $V(r_{13})$ undergoes a sharp change while $H_{13}$ changes smoothly. Thus, the $V(r_{13})$ potential energy is primarily redistributed in the Li$^+$ subsystem of electrons 1 and 3. On the other hand, $H_{13}$ and $H_{12}$ undergo a sharp change during the 12 and 13 collisions, respectively. This should be the case, since during these times it is the energy of the $H_{12}$ and $H_{13}$ subsystem, respectively, that is conserved. Note that the higher the excess energy is, the more impulsive the electron–electron collisions are, since the collision time becomes shorter and shorter compared to the time the bound electrons need to orbit around the nucleus.

## 4.2. Dominant collision sequences

For the majority of triple ionizing trajectories, we register at least two electron–electron collisions. For automated identification of the collisions sequences we need a sensitivity threshold to register only the important collisions for the triple ionizing trajectories. This is done individually for each trajectory by forming the maximum $D = \max_{i \neq j}\{|\mathbf{D}_{ij}|\}$ and normalizing each collision according to $D_{ij} \equiv |\mathbf{D}_{ij}|/D$. A collision is only registered if $D_{ij} > \delta$. The resulting classification shown in figure 4 does not sensitively depend on the exact value of $\delta$ which we have chosen to be $\delta = 1/8$.
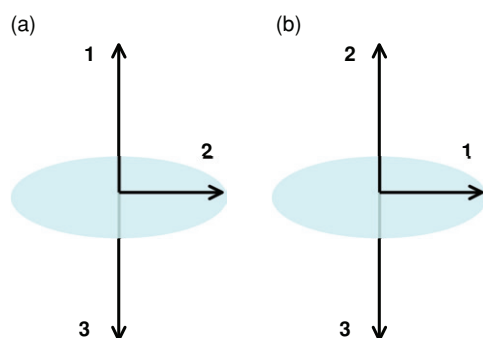
**Figure 5.** Sketch of the T-shape structure when the three electrons escape to the continuum through the $s_1$ process (a) and through the $s_2$ process (b).

(This figure is in colour only in the electronic version)

According to our classification scheme the photo-electron transfers energy to the other two electrons through two main sequences of collisions in about 84% of all triple ionization events. In the first main pathway to triple ionization, the $s_1 = (12, 13)$ sequence, the photo-electron (1) knocks out, successively, electrons 2 and 3. In the second main pathway, the $s_2 = (12, 23)$ sequence, the photo-electron 1 first knocks out electron 2. Then, electron 2 knocks out electron 3. It is easy to understand how the relative probability of these two processes is changing as a function of excess energy. The process $s_1 = (12, 13)$ has the highest weight for low excess energy where the photo-electron (after photon absorption) is still slow enough to easily transfer energy, first to electron 2 and then to electron 3. For higher energy, the competing process $s_2 = (12, 23)$ takes over because the photo-electron is still so fast after its first collision with electron 2 that the interaction with the more loosely bound 2s electron 3 is small. Rather, it is more probable that electron 2 transfers part of the energy it has gained after the initial 12 collision to electron 3 through the 23 collision.

Generally speaking, the more collisions a sequence has, the less is its weight which can be seen in figure 4 comparing the weight of $s_4$ and $s_5$ with $s_1$ and $s_2$. However, there are also exceptions, as illustrated by $s_3 = (13, 12)$. That this sequence does not carry large weight is obvious since it is not very likely that the photo-electron collides first with (2s) electron 3 and later with the more tightly bound (1s) electron 2.

### 4.3. The influence of the collision scheme on the angular correlation probability

One would expect that the collision scheme with its two dominant pathways to the continuum, the sequences $s_1$ and $s_2$, has a prominent influence on collisional observables. Indeed, as we will show, it explains the T-shaped configuration (see figure 5) of the three outgoing electrons which manifests itself in the angular correlation displayed in figure 2. To this end, we have investigated the angular correlation $C(\theta)$ in more detail by asking which angle $\theta_{ij}$ the individual electron pairs $ij$ (i.e., 12, 23, and 13) form upon leaving the nucleus. This allows us to determine the characteristic $C(\theta)$ a specific collision sequence $s_i$ produces. We show the result in figure 6 for the two dominant sequences $s_1$ and $s_2$. One sees that the electron pair which undergoes the *last* collision in a sequence (13 for $s_1$ and 23 for $s_2$) leaves towards opposite sides with an angle of $\theta = 180°$. On the other hand, the pair which collides first (12 for both sequences) forms an angle of $\theta = 90°$, and so do the pairs which do not undergo an
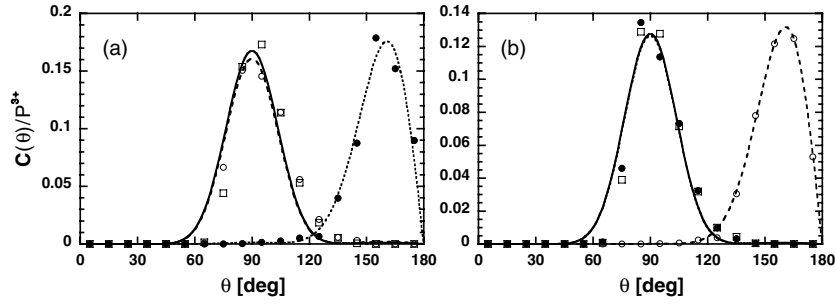
**Figure 6.** Angular correlation probability for $E = 0.9$ eV as in figure 2, but between two specific electrons 12 (open square/solid line), electrons 13 (filled circle/dotted line) and electrons 23 (open circle/dashed line). Part (a) is for trajectories from the $s_1$ sequence, part (b) for those from the $s_2$ sequence, for details, see the text.

explicit collision (23 for $s_1$ and 13 for $s_2$). The solid and dashed lines in figure 6 are fits with the functions

$$C^{ij}_\perp(\theta) = c^{ij}_\perp \sin^{\beta_\perp}\theta \sin\theta \qquad (12)$$

$$C^{ij}_\parallel(\theta) = c^{ij}_\parallel \sin^{\beta_\parallel}\theta/2 \sin\theta, \qquad (13)$$

respectively, where the $c^{ij}$ and $\beta$ are fitting parameters, while $\sin\theta$ comes from the line element of integration, $\sin\theta\,d\theta$. Taking the direction of the electron leaving in the plane perpendicular to the pair escaping back to back as a reference, it is easy to see that the average width in the distribution about $180°$ should be twice that about $90°$, i.e., $\beta_\parallel \approx 2\beta_\perp \equiv 2\beta$. This is indeed the case and all curves in figure 6 are fitted well by $\beta = 16.8$. The fits to the individual curves in figure 6 together produce the curve shown in figure 2 according to

$$C(\theta) = \sin\theta[c_\perp \sin^\beta(\theta) + c_\parallel \sin^{2\beta}(\theta/2)], \qquad (14)$$

with

$$c_\perp = c^{12}_\perp(s_1) + c^{23}_\perp(s_1) + c^{12}_\perp(s_2) + c^{13}_\perp(s_2) \qquad (15)$$

$$c_\parallel = c^{13}_\parallel(s_1) + c^{23}_\parallel(s_2). \qquad (16)$$

For the two dominant collision sequences $s_1$ and $s_2$ the T-shape geometry implies that the inter-electronic angle $90°$ is produced twice (by the first pair of electrons colliding and by the pair which does not collide) while only the pair involved in the second and last collision produces a peak at $180°$. Since the peaks at $90°$ and $180°$ for the angular correlation of individual electron pairs have roughly the same height (see figure 6) this should lead in the full angular correlation probability to a peak at $90°$ which is twice as high as that near $180°$. As one can see from figure 2 this is indeed the case.

The T-shape is the consequence of the sequential process of two collisions which dominates triple ionization since both main pathways $s_1$ and $s_2$ contain two collisions. Widely unnoticed the T-shape configuration was already mentioned in [27] for small excess energy in a model calculation of electron impact ionization of helium. The reason that this T-shape like escape has not received any attention since then lies probably in the fact that its connection to the fundamental organization of the triple escape in characteristic collision sequences of the electrons was not known until now.
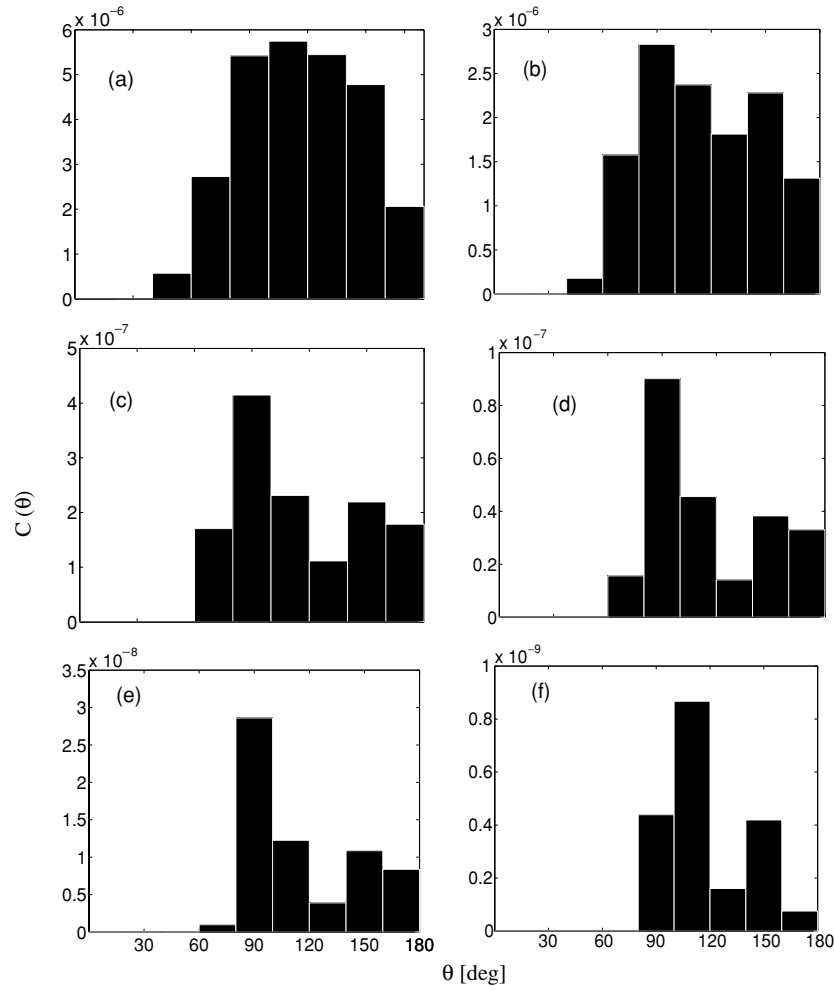
**Figure 7.** Angular correlation probability $C(\theta)$ for excess energies of $E = 10$ eV (a), 6.2 eV (b), 2 eV (c), 0.9 eV (d), 0.5 eV (e) and 0.1 eV (f). $C(\theta)$ has been binned over $20°$ at $10°, 30°, \ldots, 150°, 170°$ to reduce the statistical error. Its value for the total triple ionization probability does not exceed 3% in (a)–(e) and 10% in (f).

## 4.4. Evolution of the angular correlation distribution with excess energy

As already indicated in figure 2 the T-shape is lost towards higher energies where impulsive collisions dominate and the electrons are so fast that $\theta = 180°$ is not reached. On the other hand, approaching $E \rightarrow 0$ we expect the symmetric triangular escape according to Wannier. In our present calculation we see a clear tendency for the transition to the Wannier configuration only at the lowest excess energy (0.1 eV) we are able to calculate, see figure 7(f). This could mean that, at least concerning differential observables, the Wannier regime in triple ionization has an extremely short range in energy. It could, however, also mean that our approach, treating the photo-electron very differently from the other electrons, favours asymmetric break up of the electrons and therefore a very low transition energy between symmetric and asymmetric electron configurations.

In fact, we use a high frequency approximation for all excess energies when we let the photo-electron start after photo absorption at the nucleus ($\mathbf{r}_1 = 0$). However, as can be seen in figure 1, this leads to an excellent description of the triple ionization cross section. In additional calculations (not shown here) we have tested a frequency-dependent position of photo absorption for the photo-electron ($r_1 \propto \omega^{-1/2}$). This did not change the triple photoionization cross section for low and high excess energies and lead to small differences at intermediate energies. For simplicity and in the light of the other approximations made we have kept the high frequency approximation for the photo absorption.

We would also like to note that the simplified initial state without angular correlations does not spoil the angular correlation discussed here which depends for low and intermediate excess energies as discussed here dominantly on final state correlations which are included to all orders due to the time-dependent approach we use.

## 5. Discussion and conclusions

To summarize, we find classically that in triple ionization of lithium by single photon absorption the three electrons escape to the continuum through a dominant T-shape configuration for excess energies that are in the range of validity of the Wannier law ($\alpha = 2.16$) [10]. This T-shape configuration gives rise to a double hump structure in the inter-electronic angular distribution of the escaping electrons at $90°$ and $180°$. We have explained this surprising double hump structure in terms of a novel classification scheme that is built upon momentum transferring electron–electron collisions.

In the framework of many body perturbation theory (MPT) different ionization processes have been known for many years [28]. However, as the name already says, the perturbative character of this approach makes it applicable at high excess energies only with the electron–electron interaction treated to first or second order. The classification scheme we have developed emerges from the full classical dynamics which includes the electron–electron interaction to all orders. Surprisingly, our scheme shows that we can describe the triple photoionization process as a sequence of electron–electron collisions for energies close to threshold, where the Wannier theory becomes valid.

The sequence of collisions relevant for lithium involves only three-body helium-like subunits (nucleus and two electrons) at one instant of time. Since Coulomb systems interact via two-body forces only, it may well be that this scheme holds for more than three electrons in an atom. At the same time this would imply that not a two-electron atom but a three-electron atom is the fundamental system whose understanding allows one to access multi-electron ionization dynamics in the future. Our scheme might also guide the way to a quantum mechanical analysis along the lines of [29].

Furthermore, our study may offer valuable insight into the triple photoionization process in connection to double ionization by electron impact. For double ionization, the relationship between electron impact ionization of He$^+$ and a quasiclassical formulation of the double photoionization from the He ground state has already been established [11, 12]. Both processes differ only slightly, namely, in the energy scale set by the respective bound electron. We believe that our quasiclassical formulation of the triple photoionization of the Li ground state is a process very similar to double ionization of the excited states 1s2s $^{1,3}$S of Li$^+$ by electron impact. The target state involved is the 1s2s Li$^+$, since in the triple photoionization process the photo-electron is a 1s electron knocking out the remaining two, 1s and 2s, electrons. Experimental/theoretical results on double ionization of Li$^+$ by electron impact are needed to establish whether or not the two three-electron escape processes are indeed similar. Such results would also elucidate how the spin symmetry—not accounted for in our classical

calculation—affects the double ionization by electron impact from the excited states 1s2s $^{1,3}$S of Li$^+$.

An experimental investigation of the double hump structure we predict for the interelectronic angular distribution for small excess energies is very desirable. It could confirm the existence of the T-shaped escape of the three electrons and would thereby support our classification scheme of collisions as well as the validity and limitations of a classical approach to the four-body Coulomb problem.

## Acknowledgment

## References

[1] Colgan J, Pindzola M S and Robicheaux F 2004 *Phys. Rev. Lett.* **93** 053201
　　　Colgan J, Pindzola M S and Robicheaux F 2005 *Phys. Rev.* A **72** 022727
[2] Pattard T and Burgdörfer J 2001 *Phys. Rev.* A **63** 020701
[3] Wehlitz R, Huang M-T, DePaola B D, Levin J C, Sellin I A, Nagata T, Cooper J W and Azuma Y 1998 *Phys. Rev. Lett.* **81** 1813
[4] Wehlitz R, Pattard T, Huang M-T, Sellin I A, Burgdörfer J and Azuma Y 2000 *Phys. Rev.* A **61** 030704
[5] Carlson T A 1967 *Phys. Rev.* **156** 147
　　　Parr A C and Inghram M G 1970 *J. Chem. Phys.* **52** 4916
[6] Abrines R and Percival I C 1966 *Proc. Phys. Soc. London* **88** 861
[7] Hardie D J W and Olson R E 1983 *J. Phys. B: At. Mol. Phys.* **16** 1983
[8] Eichenauer D, Grün N and Scheid W 1981 *J. Phys. B: At. Mol. Phys.* **14** 3929
[9] Cohen J S 1985 *J. Phys. B: At. Mol. Phys.* **18** 1759
[10] Emmanouilidou A and Rost J M 2006 *J. Phys. B: At. Mol. Opt. Phys.* **39** L99
[11] Samson J A R 1990 *Phys. Rev. Lett.* **65** 2861
[12] Schneider T, Chocian P L and Rost J M 2002 *Phys. Rev. Lett.* **89** 073002
　　　Schneider T and Rost J M 2003 *Phys. Rev.* A **67** 062704
[13] Wehlitz R 2006 private communication, see also [3]
[14] Emmanouilidou A and Rost J M unpublished
[15] Rost J M 1995 *J. Phys. B: At. Mol. Opt. Phys.* **28** L601
[16] Kabir P K and Salpeter E E 1957 *Phys. Rev.* **108** 1256
[17] Emmanouilidou A, Schneider T and Rost J M 2003 *J. Phys. B: At. Mol. Opt. Phys.* **36** 2714
[18] Geyer T and Rost J M 2002 *J. Phys. B: At. Mol. Opt. Phys.* **35** 1479
[19] Heller E J 1976 *J. Chem. Phys.* **65** 1289
[20] Gaspard P 1998 *Chaos, Scattering and Statistical Mechanics* (Cambridge: Cambridge University Press)
[21] Henriksen N E 1995 *Adv. Chem. Phys.* **91** 433
[22] Kustaanheimo P and Stiefel E 1965 *J. Reine Angew. Math.* **218** 204
[23] Malcherek A W, Rost J M and Briggs J S 1997 *Phys. Rev.* A **55** R3979
[24] Wannier G H 1953 *Phys. Rev.* **90** 817
[25] Klar H and Schlecht W 1976 *J. Phys. B: At. Mol. Phys.* **9** 1699
[26] Dimitrijevic M S and Grujic P 1981 *J. Phys. B: At. Mol. Phys.* **14** 1663
[27] See, for example, McGuire J H 1997 *Electron Correlation Dynamics in Atomic Collisions* (Cambridge: Cambridge University Press) and references therein
[28] Briggs J S 1990 *Phys. Rev.* A **41** 539